Analysis of the chaotic behaviour of orbits diffusing along the Arnold web

Claude Froeschlé (claude@obs-nice.fr) [(1)], Elena Lega (elena@obs-nice.fr) [(1)] and Massimiliano Guzzo (guzzo@math.unipd.it) [(2)]

[(1)] *Observatoire de la Côte d'Azur, B.P. 4229, 06304 Nice Cedex 4 (France)*

[(2)] *Dipartimento di Matematica pura e Applicata Università di Padova, Via Belzoni 7, 35131 Padova (Italy)*

Abstract. In a previous work (Guzzo, Lega and Froeschlé, DCDS B Vol.5, 687-698, 2005) we have provided numerical evidence of global diffusion occurring in slightly perturbed integrable Hamiltonian systems and symplectic maps. We have shown that even if a system is sufficiently close to be integrable, global diffusion occurs on a set with peculiar topology, the so–called Arnold web, and is qualitatively different from Chirikov diffusion, occurring in more perturbed systems. In the present work we study in more detail the chaotic behaviour of a set of 90 orbits which diffuse on the Arnold web. We find that the largest Lyapunov exponent does not seem to converge for the individual orbits while the mean Lyapunov exponent on the set of 90 orbits does converge. In other words, a kind of average mixing characterizes the diffusion. Moreover, the Local Lyapunov Characteristic Numbers (LLCNs), on individual orbits appear to reflect the different zones of the Arnold web revealed by the Fast Lyapunov Indicator. Finally, using the LLCNs we study the ergodicity of the chaotic part of the Arnold web.

Keywords: KAM and Nekhoroshev theorem, Arnold's diffusion, chaos detection

1. Introduction

The characterization of mechanisms for diffusion of orbits in quasi–integrable Hamiltonian systems and symplectic maps is a relevant topic for many fields of physics, such as celestial mechanics, dynamical astronomy (Vergassola 1998, Contopoulos 2002, Morbidelli 2002) , statistical physics, plasma physics and particle accelerators. Any dynamical state of an integrable system can be characterized with a set of action–angle conjugate variables where the actions are constants of motion, while the angles simply change linearly with time. The properties of the system which are relevant for the stability are determined by the actions.

Small perturbations of integrable systems can produce a slow drift of the initial value of the actions, and after certain time these drifts can cumulate in such a way to drive the orbit far away its initial value.

In 1979 Chirikov described (Chirikov 1979) a possible model for global drift valid when the perturbation is greater than some critical value. One of the reasons of the broad detection of the Chirikov diffusion is that its typical times fall within the simulation abilities of modern computers as far back as the seventies.

For smaller perturbations the systems fall within the range of celebrated perturbation theories such as KAM (Kolmogorov 1954, Moser 1958 and Arnold 1963) and Nekhoroshev (1977) theorems which leave the possibility for global drift only on a subset of the possible dynamical states with peculiar topology, the so–called Arnold web, and force diffusion times to be at least exponentially long with an inverse power of the norm of the perturbation. Following Nekhoroshev (1977), we call Arnold diffusion a diffusion occurring on the Arnold web of a system which satisfies the hypotheses of both KAM and Nekhoroshev theorems.

The theoretical possibility of Arnold diffusion has been first shown by Arnold (1964) for a specific system.

Being interested to applications to specific systems, and in particular to systems of interest for physics, we have used a numerical approach (Lega et al. 2003, Guzzo et al. 2005)

which, avoiding theoretical difficulties, measures directly the quantitative features of long term diffusion. More precisely, we consider systems satisfying the hypothesis of both KAM and Nekhoroshev theorems and small values of the perturbation parameter so that both theorems apply. Therefore, beyond estimates of diffusion and instability we provide a direct numerical investigation of the geometry of the resonances of the system (Froeschlé et al. 2000) which clearly allows to identify the dynamical regime in which the diffusion is detected.

Following this strategy, we detected (Lega et al. 2003) a very slow local diffusion confined to the Arnold web of a system which satisfies both the hypotheses of KAM and Nekhoroshev theorems. In that work, we estimated the diffusion coefficient to decrease faster than a power law of the perturbing parameter, consistently with the exponential estimates provided by the Nekhoroshev theorem. More recently, we have provided evidence that indeed those orbits diffuse in macroscopic domains of the action space (Froeschlé et al. 2005, Guzzo et al. 2005).

In the present paper we analyze the chaotic behaviour of such orbits. We show that the largest Lyapunov exponent does not seem to converge for the individual orbits while the mean Lyapunov exponent on a set of 90 orbits does converge. We have computed the Local Lyapunov Characteristic Numbers (Froeschlé et al. 1993, LLCNs hereafter) [1] on individual orbits showing that their values reflect the different zones of the Arnold web.

Considering an ergodic approach, we test the equivalence between spatial and temporal averages in the chaotic part of the Arnold web. Of course, the ergodic hypothesis is trivially not valid if we consider generic open sets in the phase space, because of the existence of the invariant tori. Instead the ergodic hypothesis could be potentially true if we restrict it to the subset of the phase space with Fast Lyapunov Indicator (FLI hereafter,introduced in Froeschlé et al. 1997, defined here in Section 2, Eq.3) higher that the FLI which characterizes the KAM tori. Even in this case, what we find is that the equivalence between spatial and temporal averages is not so evident even for large values of the perturbation parameter.

In Section 2 we describe the geometry of the Arnold web of symplectic maps and we recall the numerical method used to detect the Arnold web and the global diffusion on it. We report in Section 3 the computation of the Largest Lyapunov Exponent of orbits diffusing on the Arnold web and we recall the definition of the Local Lyapunov Characteristic Numbers showing how they are related to the geography of the resonances.

In Section 4 we look for the application of the ergodic hypothesis for different values of ϵ. Conclusion is provided in Section 5.

2. Numerical detection of the Arnold web

We consider the following quasi–integrable symplectic map:

$$\begin{cases} \phi_1' = \phi_1 + I_1 & , \quad \phi_2' = \phi_2 + I_2 \\ I_1' = I_1 + \epsilon \frac{\partial f}{\partial \phi_1}(\phi_1 + I_1, \phi_2 + I_2) & , \quad I_2' = I_2 + \epsilon \frac{\partial f}{\partial \phi_2}(\phi_1 + I_1, \phi_2 + I_2) \end{cases} \tag{1}$$

where $f = 1/(\cos(\phi_1) + \cos(\phi_2) + 4)$. At small ϵ, the KAM and Nekhoroshev theorems (Kuksin 1993, Kuksin and Pöschel 1994, Guzzo 2004) apply to this kind of maps. The resonances of this system are defined by the straight lines $k_1 I_1 + k_2 I_2 + 2\pi k_3 = 0$, with $k_1, k_2, k_3 \in \mathbb{Z}\backslash 0$. To describe the topology of the Arnold web, it is convenient to refer to the subset of the phase space determined by the section $S = \{(I_1, I_2) \in \mathbb{R}^2, \phi_i = 0, i = 1, 2\}$. From the KAM theorem, it follows that any invariant torus cuts the section S in only one point (I_1, I_2). Moreover, the

[1] Sometimes called stretching numbers (Voglis and Contopoulos 1994)

Diophantine condition on the frequencies implies that these points are outside a neighborhood of lines $k_1 I_1 + k_2 I_2 + 2\pi k_3 = 0$ proportional to $\gamma/|k|^\tau$, for any $k = (k_1, k_2, k_3) \in \mathbb{Z}^3 \backslash 0$. Therefore, the intersection between the Arnold web and the section S consists of all these straight lines with a neighborhood which decreases as $|k|$ increases. Any of these straight lines is called resonance, and the integer $|k|$ is called resonance order. The Arnold web is open, dense, and has a small relative measure (proportional to γ).

A precise numerical detection of the Arnold web is possible with the so-called Fast Lyapunov Indicator (hereafter, FLI) method (Froeschlé et al. 1997, Froeschlé et al. 2000).

The FLI is related to the computation of the tangent map for a given choice of an initial tangent vector and was first introduced to detect weak chaos (Froeschlé et al. 1997).

We recall that given a set of differential equations:

$$\frac{d}{dt}\vec{X} \;=\; \vec{F}(\vec{X}) \;\;,\;\; \vec{X} = (x_1, x_2 .... x_n) \tag{2}$$

under some suitable regularity conditions, the evolution $\vec{v}(t)$ of any vector $\vec{v}(0) \in R^n$ is obtained by integrating the variational equations:

$$\frac{d\vec{v}}{dt} = (\frac{\partial \vec{F}}{\partial X})\vec{v} \;\;.$$

The largest Lyapunov exponent is defined in such a way that, unless $\vec{v}(0)$ belongs to some lower dimensional linear spaces, the quantity $\ln ||\vec{v}(t)||/t$ tends to it as t goes to infinity. Of course numerically we work on finite times and we call Lyapunov Characteristic Indicator the quantity $\ln ||\vec{v}(t)||/t$ at a given time t. If equation (2) is Hamiltonian and if the motion is regular (except for some peculiar hyperbolic structures, such as whiskered tori) then the largest Lyapunov exponent is zero, otherwise it is positive. This property has been largely used to discriminate between chaotic and ordered motion. However, among regular motions the Lyapunov exponent does not distinguish between KAM tori and regular resonant motions.

We recall that the FLI (Froeschlé et al. 2000, Guzzo et al. 2002) is defined as:

$$FLI(t) = \sup_{0<k<t} \log ||v(k)|| \tag{3}$$

As detailed in (Guzzo et al. 2002) the FLI distinguishes between resonant and non resonant regular motions.

In (Guzzo et al. 2005) we showed that the Arnold web of the above mapping indeed corresponds to the above theoretical description. Moreover we have shown how to choose initial conditions which are good candidates to diffuse thanks to the accurate detection of the web. In fact, within resonances, both chaotic and regular motions are observed. Of course, regular motions do not diffuse, and therefore diffusive orbits must be chosen in the small subset of the Arnold web made of chaotic motions. We are aware that the set of chaotic orbits selected (having FLI larger than the reference value for the tori) could include periodic orbits with very large periods which formally do not diffuse but numerically seem to diffuse. Anyway the measure of such orbits is close to zero.

Moreover, even within chaotic motions, to have the chance to observe the phenomenon one has to restrict the choice of initial conditions to the single order resonances, i.e. to the portion of resonant lines which are far from the main crossing between resonances. The reason is that stability times are expected to be much longer up to a distance of order $\sqrt{\epsilon}$ from these crossings (see, for example, Pöschel 1993). With this selection of initial conditions, we have been able to show, in Lega et al. (2003), that indeed after times that increase faster than power law, initial conditions diffuse along the chaotic border of resonant lines. Though the computational time

used in Lega et al. (2003) was already quite long, due to the slowness of Arnold diffusion, it was not sufficient to evidence a global instability and diffusion, i.e. the wandering of motions from one resonance to the others. Thanks to a much longer computational time, and the use of a suitable symplectic map, we have displayed in (Froeschlé et al. 2005 and Guzzo et al. 2005) for the first time a global diffusion phenomenon.

Fig.1 shows the Arnold web detected computing the FLI of the mapping 1 for $\epsilon = 0.6$ on a set of 500×500 initial conditions taken on section S and regularly spaced in I_1, I_2.

In the plot, we have associated to each point of the action plane (I_1, I_2) a color corresponding to the FLI value according to the color scale reported below the figure[2]. The intermediate value of the FLI (grey in the color scale) corresponds to KAM tori. Darker regions correspond to initial conditions (I_1, I_2) on the section S which produce resonant regular motions, while light grey regions correspond to initial conditions which produce chaotic motions. Each resonance appears as a darker grey region with a light grey border, or as a single light grey line (depending on the resonance and on the value of the angles chosen to define the section S; see Froeschlé et al. 2000 for more details). Therefore, the light grey region on the FLI map corresponds to the chaotic subset of the Arnold web, where an eventual Arnold diffusion should be confined.

Following the explained criterion of choice of the initial conditions we have repeated the computation of Guzzo et al. (2005) on a larger set (90 instead of 20) of initial conditions near $(I_1, I_2) = (2.35, 1.07)$. Then, we computed numerically the map up to $2\,10^{10}$ iterations. The results are reported in the four panels of Figure 1 : on the FLI map of the action plane (I_1, I_2) we plotted as black dots all points of the orbits which have returned after some time on the section S. Of course, because computed orbits are discrete we represented points on the double section $|\phi_1| \leq 0.005$, $|\phi_2| \leq 0.005$; reducing the tolerance 0.005 reduces only the number of points on the section, but does not change their diffusion properties. Figure 1a shows the local diffusion along the resonance $I_1 = 2I_2$, while figure 1b shows the result after the intermediate time $2\,10^8$. We observe that the orbits diffuse also along resonant lines different from the initial one.

Figure 1c,d show the result after much longer times. To properly display such long term evolutions we used a zoomed out map of the action plane.

We observe that the orbits filled a macroscopic region of the action plane whose structure is clearly that of the Arnold web. The orbits have moved along the single resonances, and avoided the center of the main resonance crossings, in agreement with the theoretical results which predict longer stability times for motions in these regions. The larger resonances (which correspond to the smallest orders $|k|$) are practically all visited, while this is not the case for the thinest ones (which correspond to the highest orders $|k|$). This is in agreement with the theoretical results of Morbidelli and Giorgilli (1995), which predict that the speed of diffusion on each resonance becomes smaller for resonances of high order. Therefore, the possibility of visiting all possible resonances is necessarily limited by finite computational time.

In figure 2 we plotted the orbits corresponding to two very close initial conditions. The figure allows to appreciate that, although the differences in the initial actions is only 10^{-4}, the two orbits undergo completely different paths. In order to estimate the precision of the calculation we have integrated over 10^{11} an initial condition corresponding to a KAM torus finding that the supremum of the variation of the actions, on the double section S, with respect to their initial value is of the order of 10^{-4}. Moreover, the integration of chaotic orbits of a 2 degree of freedom Hamiltonian didn't show a diffusion (E. Lega 2002, Thèse d'Habilitation à diriger des recherches) violating the conservation of energy.

[2] Color pictures can be found at:*http://www.obs-nice.fr/elena/Global_diffu/images.html*

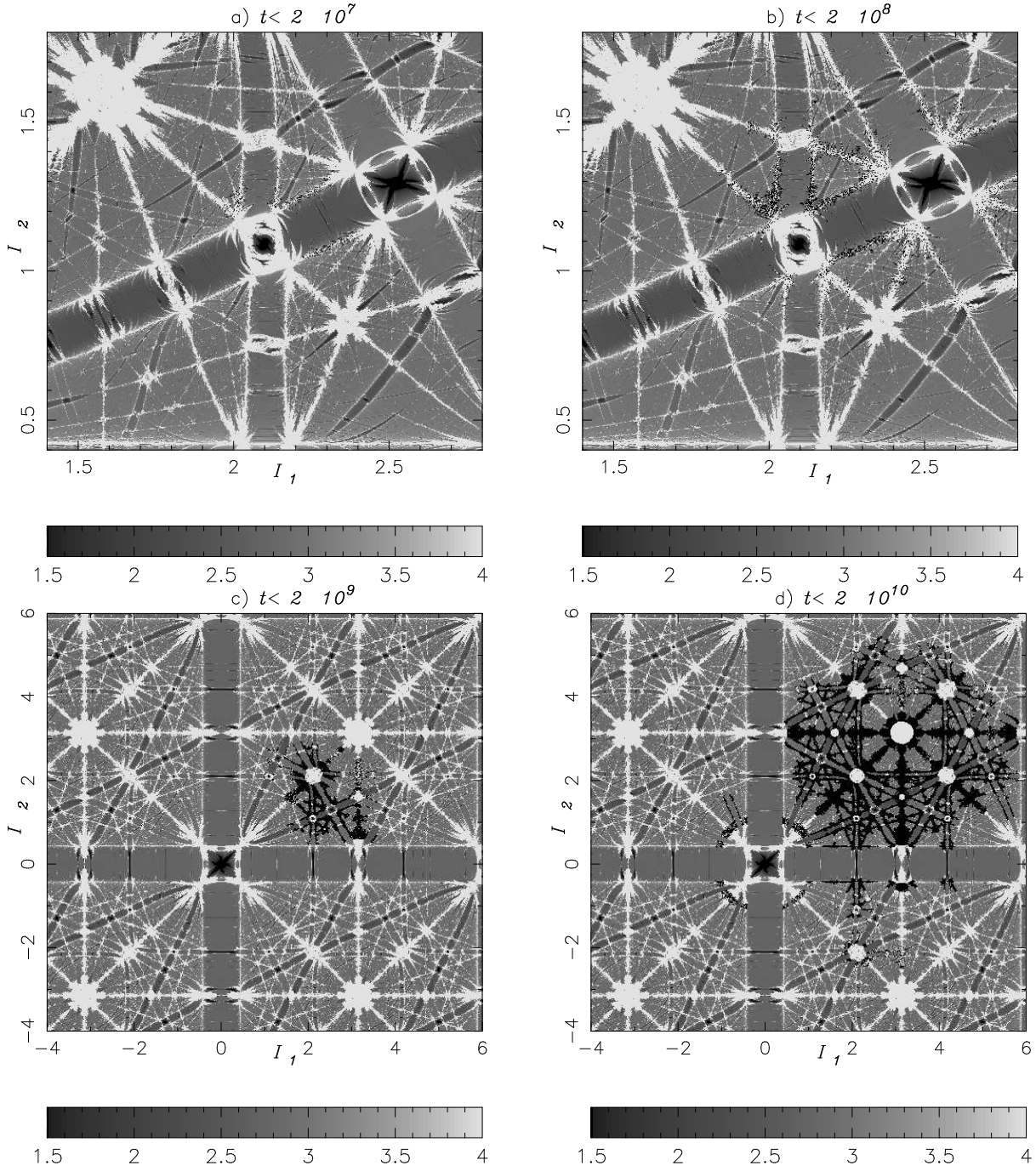

Figure 1. The four panels correspond to the FLI map of the action plane (I_1, I_2) for the map (1), with initial condition on the section S, with different magnifications. The light grey region corresponds to the chaotic part of the Arnold web. On panel (a,b,c,d) we mark with a black dot all points of the 90 orbits which have returned after some time on the section S. We consider $2\,10^7$ iterations for panel (a); $2\,10^8$ iterations for panel (b), $2\,10^9$ iterations for panel (c) and $2\,10^{10}$ iterations for panel (d).

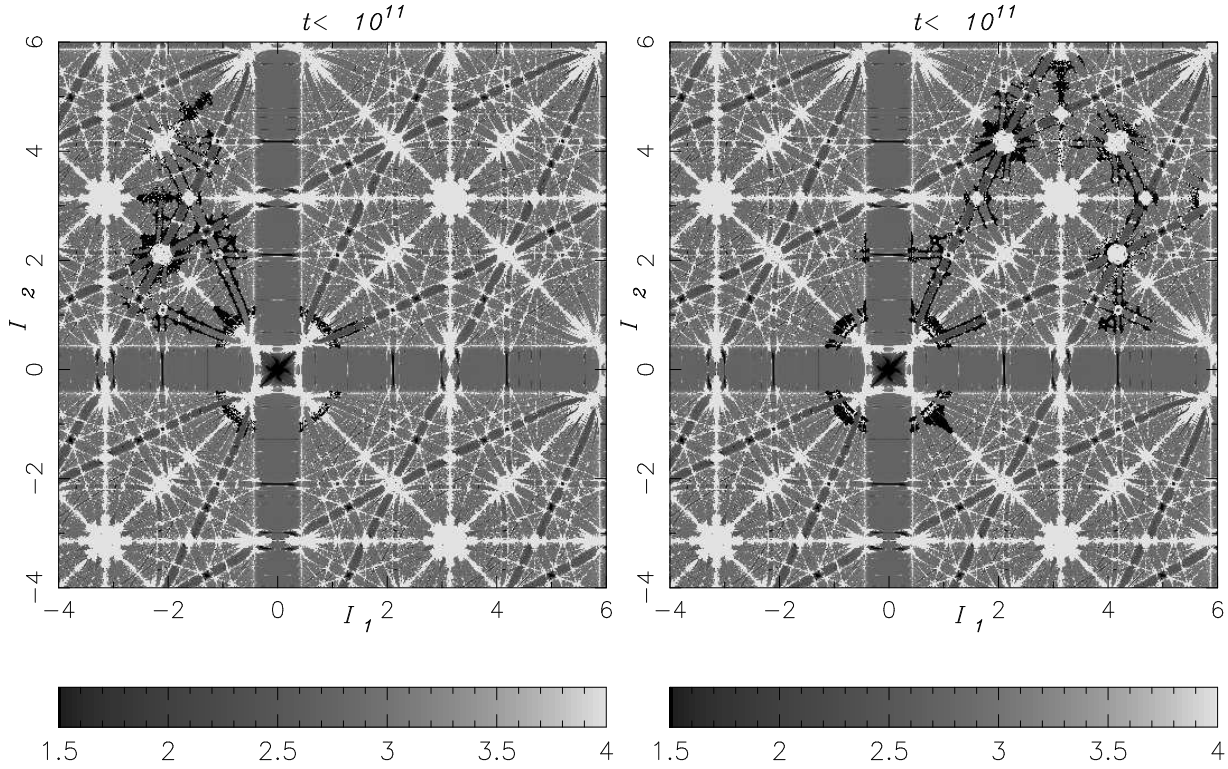

Figure 2. The two panels correspond to the FLI map of the action plane (I_1, I_2) for the map (2), with initial condition on the section S. The light grey region corresponds to the chaotic part of the Arnold web. The different panels correspond to the intersections with section S up to a time $t = 10^{11}$ of two orbits with initial conditions on the resonant line $I_1 = 2I_2$. More precisely, left panel represent the evolution of one orbit with initial conditions $I_1(0) = 1.71640$ and $I_2(0) = 0.8160$, while the right panel shows the evolution of one orbit with initial conditions $I_1(0) = 1.71643$, $I_2(0) = 0.8159$. Let us remark that although the initial conditions are very close the two orbits undergo completely different paths.

3. The Largest Lyapunov Exponent

A classical way to quantify the strength of chaos is to compute the largest Lyapunov characteristic exponent (LCE hereafter). It is well known that the LCE is defined as:

$$\lambda = \lim_{N\to\infty} \frac{1}{Nk} \sum_{n=1}^{N} \log\left(\frac{||v(nk)||}{||v((n-1)k)||}\right) \quad . \tag{4}$$

In the practical computation of λ, the vector v is renormalized every k iterations.

Let us also recall the definition (Froeschlé et al. 1993) of the Local Lyapunov Characteristic Numbers (LLCNs) as the set of numbers

$$\alpha(n) = \frac{1}{k} \log\left(\frac{||v(nk)||}{||v((n-1)k)||}\right)$$

For a given interval of time the mean of the LLCNs is nothing but the Lyapunov Characteristic Indicator (LCI hereafter) whose limit when the time goes to infinity is the LCE.

Fig.3,left shows the evolution with time of the LCI of the 2 orbits of Fig.2. We clearly observe that not only the two LCI are different but also they do not show clear convergence up to $t = 10^{11}$ iterations. However, Fig.3,right showing the evolution of the LCI of 20 orbits

whit-in the set of 90 of Fig.1 displays excursions of the LCIs whit-in a constant interval $[10^{-3}, 10^{-2}]$ for t going from 10^7 to 10^{11}. This is corroborated by the fact that the mean value of the 90 LCIs shows convergence (Fig.3,right thick line). Moreover, let us remark that the quantity $\log ||v(t)||/t$, when computed on a single stochastic region, converges to the largest Lyapunov Exponent in a time called the Lyapunov time; while it does not converge (even on a very large interval of time: $T = 10^{11}$ iterations, Fig.3) when the diffusion occurs on the Arnold web. However, Fig.3,right shows that the mean on a set of N orbits converges on a time shorter than $T/N \simeq 10^9$. Therefore, in order to compute the LCI one has to do it on a set of orbits instead that on a single one.

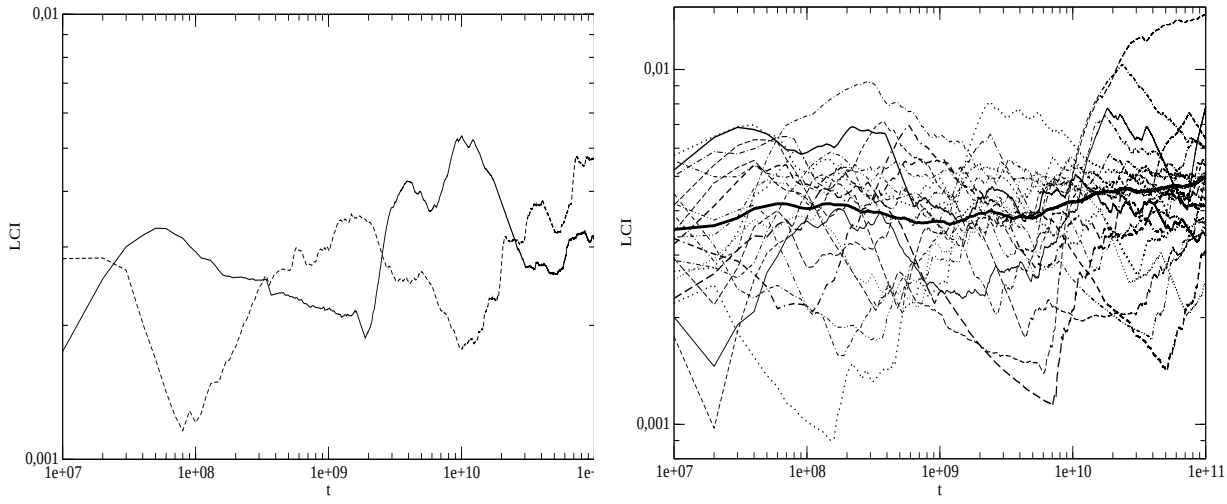

Figure 3. (left panel) Evolution with time of the LCI of the two orbits of Fig.2. (right panel). Evolution with time of the LCI of 20 of the 90 orbits of Fig.1. The more regular curve (thick line) is the evolution with time of mean value of the 90 LCI.

3.1. On the relationship between LLCNs and phase space

When computing the LCI only the mean value of the tangent vectors is considered while the distribution of such vectors can give hints about the history of the orbit. In order to explore the complex chaotic evolution of an orbit we consider first the distribution of the LLCNs of the orbit of Fig.2,left.

Fig.4 shows the distribution of the LLCNs for this orbit. Let us remark that, for a KAM torus at the same value of the perturbation parameter $\epsilon = 0.6$ the LLCNs range in the interval $[-5\,10^{-5}, 5\,10^{-}5]$. For the chaotic orbit the majority of the LLCNs range from $[2\,10^{-}5, 10^{-}3]$ and a queue of larger but rare values goes up to $1.75\,10^{-2}$. In order to see if there is a relation between the LLCNs and the motion of the orbit we have associated to the points of the orbit intersecting S the corresponding LLCNs and plotted in Fig.5,left the points having LLCNs$<$ 0.005 and in Fig.5,right the points having LLCNs$\geq$ 0.005. It appears clearly that the larger values of the LLCNs are associated to the neighbourhood of resonance crossing while the lower values

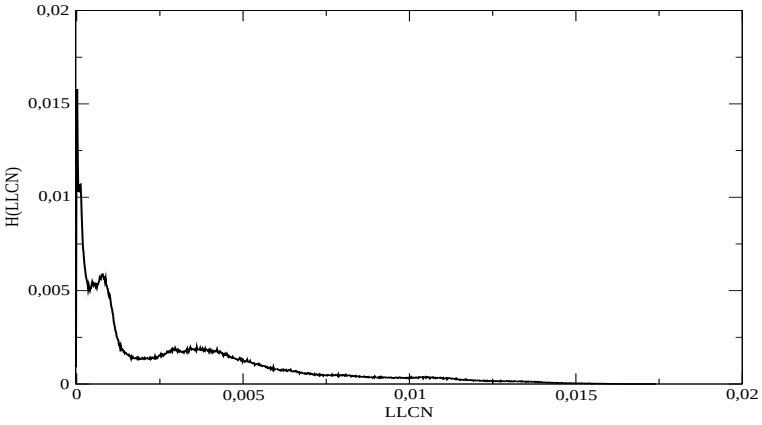

Figure 4. Distribution of the LLCNS of the orbit of Fig.2,left.

correspond to resonant lines. The great percentage of low LLCNs values is significative of the long time of residence on the resonant lines. The distribution gives informations about the different regions of the phase space visited by the orbits.

4. An ergodic approach

The aim of this Section is to revisit the old idea that in a chaotic zone all orbits have the same LCE (Contopoulos, 2002 pag.255) and that it can be computed using a set of different orbits. At this purpose, we have considered a set of 100 orbits with initial conditions in the chaotic domain taken at random in the interval $0 < I_1 < \pi$, $0 < I_2 < \pi$ ($\phi_1 = 0$, $\phi_2 = 0$) and we have integrated them for 10^8 iterations computing the LLCNs every 10^4 iterations. Considering an ergodic approach, i.e. the well known hypothesis which states the equivalence between spatial and temporal means, we have integrated one orbit of the previous set for 10^{10} iterations computing the LLCNs every 10^4 iterations.

Since the distribution of the LLCNs are closely related to the detailed chaotic history of an orbit (Fig.5) we consider the distance between the distributions of the LLCNs as a good indicator of ergodicity. More precisely,we introduce the chi squared distance:

$$d = \sum_{h=1}^{M} (P_h - \tilde{P}_h)^2 \tag{5}$$

where P_h is the percentage of LLCN's in the bin h, $h = 1, ..., 1000$ of the distribution of the LLCNs of the 100 orbits (Data set 1 in the following) and $\tilde{P}_h$ is the same as P_h for the single orbit (Data set 2 in the following).

Fig.6(dashed line) shows the variation of d as a function of the perturbation parameter ϵ.

The distance, although noisy, drops from 10^{-2} to about 10^{-4} for ϵ going from 0.5 to 1.3. For greater values of ϵ, when the system is in Chirikov regime, the distance shows noisy variations around $5\,10^{-5}$ up to $\epsilon = 9.8$. The result for large value of the perturbation parameter is puzzling. For large values of ϵ we have large chaotic domains and we expected that the orbits

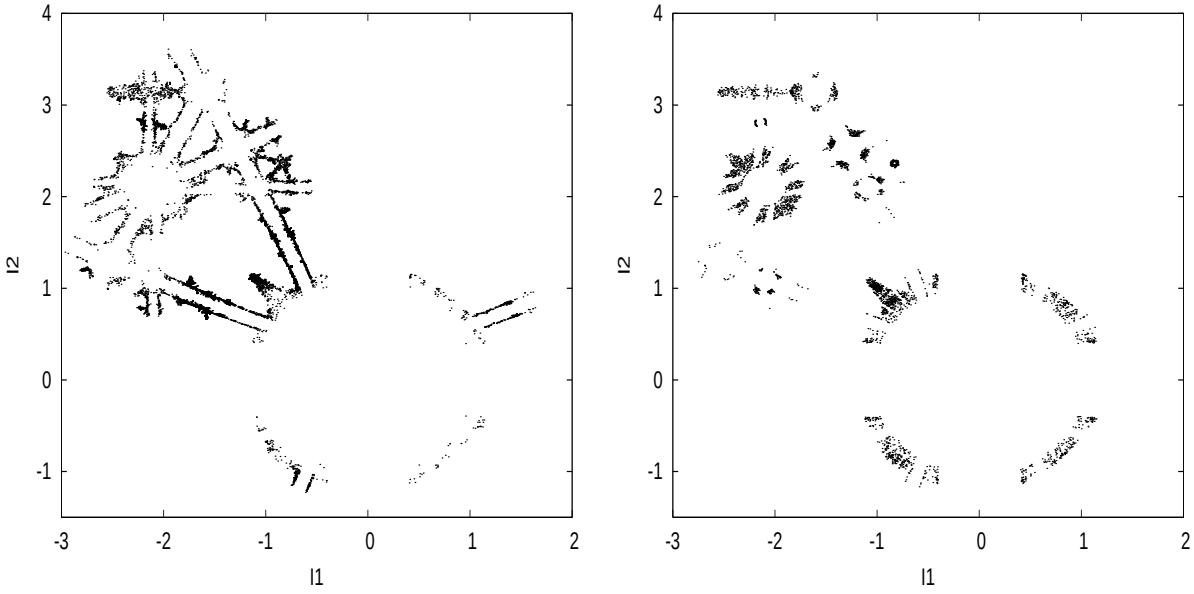

Figure 5. In the two panel the intersections of the point of the orbit of Fig.2 (left) with the section S are plotted. More precisely the points intersecting S and having $LLCN < 0.005$ are plotted in left panel the others in the right panel.

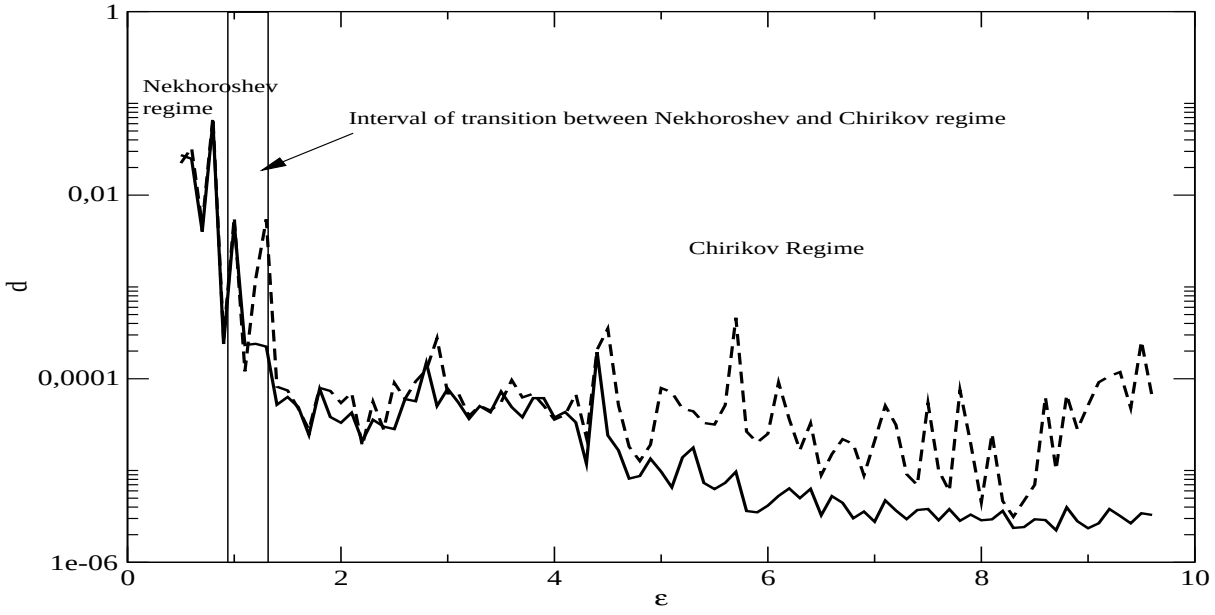

Figure 6. variation of the distance d as a function of ϵ. All points of data set 1 and data set 2 are considered (dashed line). Only 90 orbits of data set 1 and 90 sets of data set 2 having similar mean values of the LLCNs have been analyzed (continuous line). The interval $0.9 < \epsilon < 1.3$ correspond to the transition between the Nekhoroshev and the Chirikov regime.

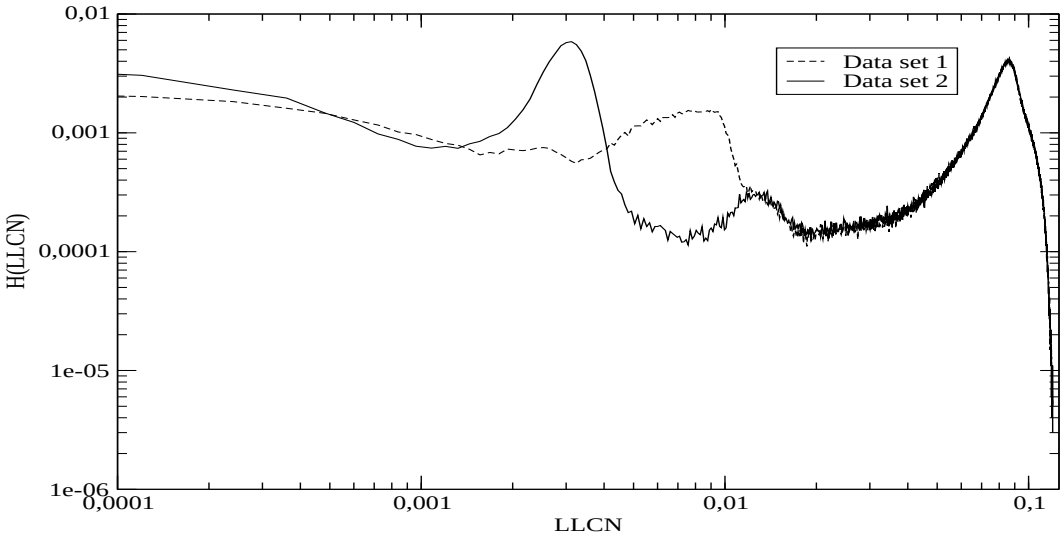

Figure 7. Histogram of the distribution of the LLCNs for data set 1 (100 orbits integrated for 10^8 iterations) and data set 2 (1 single orbit integrated for 10^{10} iterations).

of the two data sets had the same chaotic properties. To clarify the situation we have focused the attention on one case, let's say $\epsilon = 9.5$. When looking at the 2 distribution for such value of ϵ, Fig.7 shows that the difference takes place at very low values of the LLCNs.

Following the same approach than in Fig.5 we plot the points of section S having LLCNs larger than 0.01 in Fig.8,left; and those having LLCNs lower than 0.01 in Fig.8,right for the orbit of data set 2.

At first glance, in opposition to the previous case, no difference appears between the two sets of points. More precisely, there is a difference in the density distribution of the points but no structures appear neither in the left nor in the right picture, mainly because of the large domain on which the fast Chirikov diffusion takes place.

The computation of the FLI in a small portion of the phase space (indicated by a square in Fig.8,left), allows to show the presence of some regular orbits. We observe that the points having low values of the LLCNs (superimposed in black in Fig.9) lie in a close neighbourhood of regular orbits.

This phenomenon, called sticking, has been extensively studied (Contopoulos 2002 and references therein) . In addition we observe here an orbit which does not start in a sticking region but is trapped as time goes on. For two dimensional maps this is more rare. According to the theory (Morbidelli and Giorgilli 1995) the time of capture in these regions may be very long (we have found $\simeq 1/10$ of the total integration time for the analyzed orbit). One way of selecting the sticked orbits is to consider the mean values of the LLCNs of the 100 orbits (data set 1) and of the 100 sets of 10^8 iterations of the single orbit (data set 2) as shown in Fig.10 for $\epsilon = 9.5$.

It appears that the 90% of the mean values of the LLCNs are very similar while the remaining 10% are up to an order of magnitude lower.

Let us recall that the mean of the LLCNs is nothing but the LCI and we obtain very similar values when considering respectively data set 1 and 2. However, if we consider the distribution of the LLCNs the discrepancies can be removed getting rid of the sticking parts.

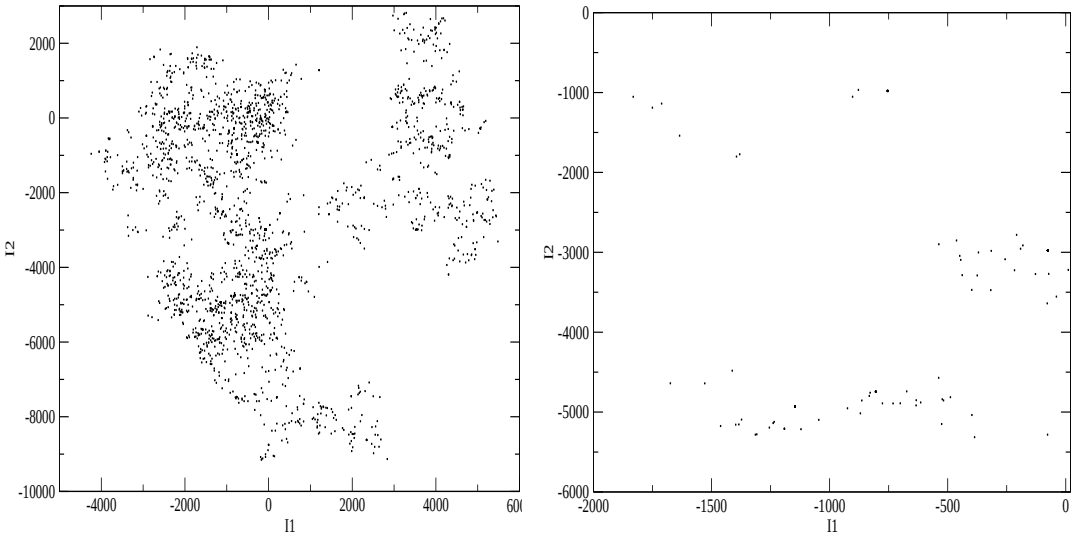

Figure 8. In the two panel the intersections of the point of the orbit of data set 2 with the section S are plotted. More precisely the points intersecting S and having $LLCN < 0.01$ are plotted in left panel the others in the right panel.

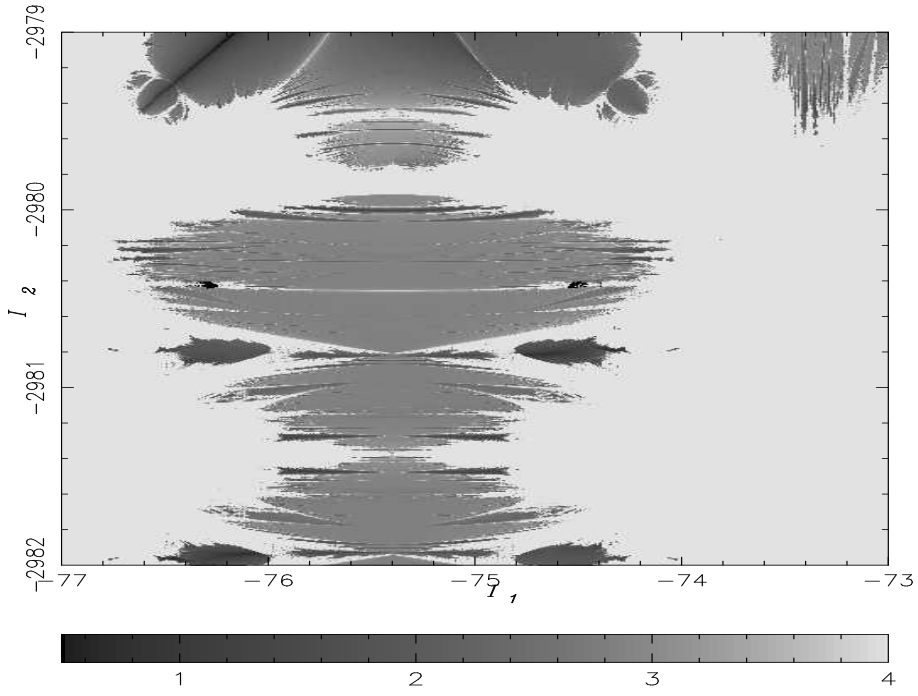

Figure 9. FLI chart of the zone of the phase space whit-in the box of Fig.8. The points of the orbit of data set 2 intersecting the section S and having LLCN$<$ 0.01 are plotted in black. They appear as two spots at about $I_2 \simeq -2980.5$ lying in a close neighbourhood of regular orbits.

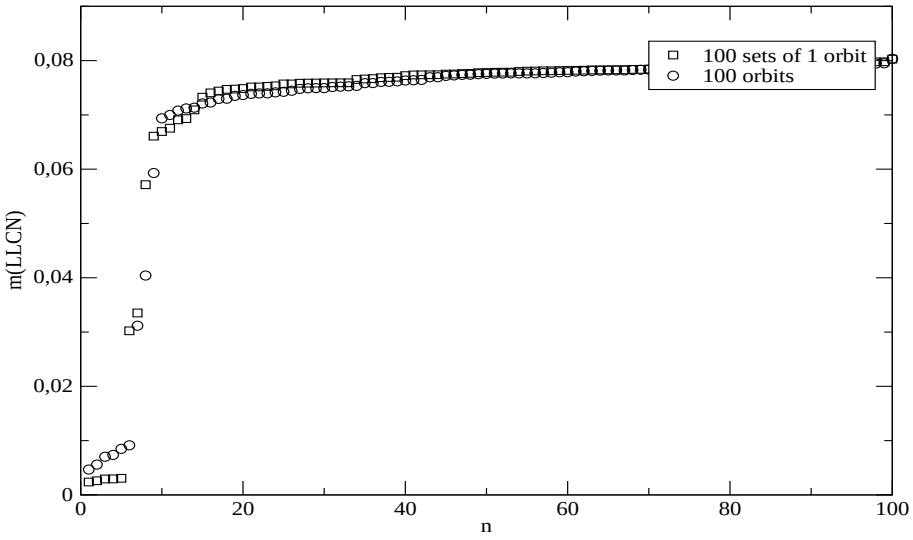

Figure 10. Mean values, ordered from minimum to maximum value, of the distributions of the LLCNs of the 100 orbits (data set 1) and of the 100 sets of 10^8 iterations of the single orbit (data set 2) for $\epsilon = 9.5$.

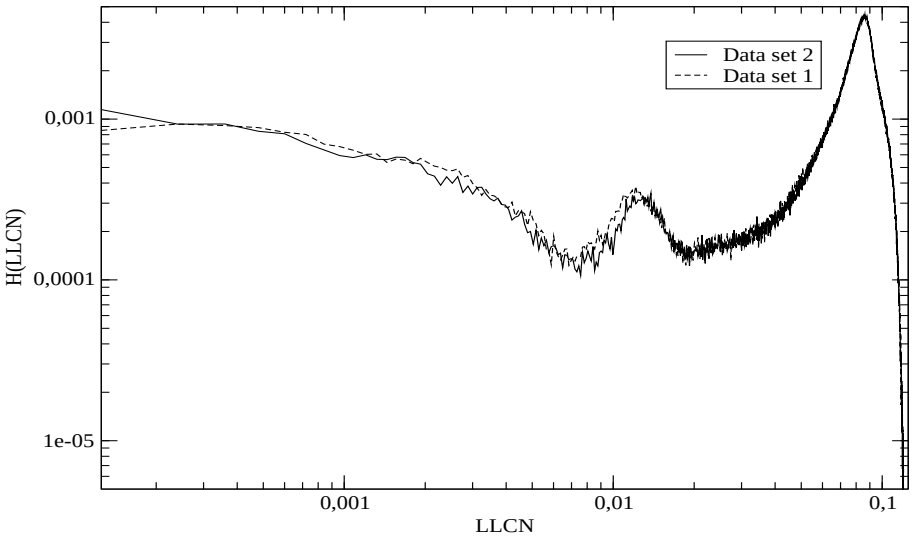

Figure 11. Histogram of the distribution of the LLCNs of data set 1 (90 orbits selected as explained in the text) and of data set 2 (90 sets of the single orbit selected as explained in the text).

The distribution of the 2 data sets containing the 90 orbits though selected appear much more similar (Fig.11).

The same procedure applied to the whole set of values of ϵ shows that, at least for large values of ϵ the noise is reduced and the values of d have decreased (Fig.6,continuous line). Finally, for low values of ϵ (Nekhoroshev regime and local Chirikov regime) we observe that even when removing the orbits, as explained above, the distance between the two sets doesn't change.

This is a consequence of the existence, for such low values of ϵ of the Arnold web structure. More precisely, some initial conditions in the crossing of resonances do not diffuse.

According to the theory (Pöschel 1993) such regions have stability times longer than in the single resonance.

Of course such results are time depending, some orbits which show intermittent phenomena with long time sticking may finally appear ergodic for a much larger time interval. We have shown that for this mapping two phenomena of complete different nature give the same macroscopic results as far as diffusion is concerned. On one side, we have the well known sticking phenomena extensively studied for two dimensional mappings and on the other side the trapping into effective stable chaotic crossing. The first phenomena is characterized by very low values of the LLCNs while the second one exhibits relatively large LLCNs. For orbits, i.e. region of the phase space which do not have such peculiar geometry, we have found an ergodic-like behaviour.

5. Conclusion

Using the FLI method, we have recalled some previous results showing evidence of global diffusion occurring in slightly perturbed systems.

In the present paper we have studied in more detail the chaotic behaviour of orbits diffusing on the Arnold web. We have shown that the LCI of such orbits does not converge on a quite long interval of time (10^{11}) iterations. However, the mean value of the LCI of the 90 explored orbits does converge showing a kind of average mixing.

Thanks to the computation of the Local Lyapunov Characteristic Numbers we were able to associate the LLCNs to geometrically well defined regions of the phase space. Moreover, we have tested the ergodicity of the system for increasing values of the perturbation parameter. We have shown that the existence of the Arnold web structure prevents ergodicity on the large but finite time $t = 10^{10}$ iterations. Conversely, for large values of the perturbation parameter, temporal and spatial means are more close, although the existence of some sticking phenomena.

References

V.I. Arnold. Proof of a theorem by A.N. Kolmogorov on the invariance of quasi-periodic motions under small perturbations of the Hamiltonian. *Russ. Math. Surveys.*, **18**:9–36, (1963).

V.I. Arnold. Instability of dynamical systems with several degrees of freedom. *Sov. Math. Dokl.*, **6**:581–585, (1964).

G. Contopoulos. Order and Chaos in Dynamical Astronomy. Springer-Verlag Berlin Heidelberg (2002).

B.V. Chirikov. An universal instability of many dimensional oscillator system. *Phys. Rep.*, **52**:263–379, (1979).

C. Froeschlé,Ch. Froeschlé, E. Lohinger. Generalized Lyapunov Characteristics Indicators and Corresponding like Entropy of the Standard Mapping, *Celest. Mech. and Dynamical Astron.*, **56**:307–315, (1993).

C. Froeschlé, M. Guzzo and E. Lega. Graphical evolution of the Arnold web: from order to chaos. *Science*, **289**:2108–2110 (2000).

C. Froeschlé, E. Lega and R. Gonczi. Fast Lyapunov Indicators. Application to Asteroidal Motion, Celest. Mech. and Dynam. Astron., **67**,41-62,1997.

C. Froeschlé,M.Guzzo, E. Lega Local and global diffusion along resonant lines in discrete quasi–integrable dynamical systems. Celest. Mech. and Dynam. Astron., **92**, 243-255, 2005.

M. Guzzo. A direct proof of the Nekhoroshev theorem for nearly integrable symplectic maps. *Annales Henry Poincaré*, **5**:1013–1039, (2004).

M. Guzzo, E. Lega and C. Froeschlé. On the numerical detection of the effective stability of chaotic motions in quasi-integrable systems. *Physica D*, **163**:1–25 (2002).

M. Guzzo, E. Lega and C. Froeschlé. First numerical evidence of global Arnold diffusion in quasi-integrable systems. *DCDS-B*, **5**,687–698,(2005).

A.N. Kolmogorov. On the conservation of conditionally periodic motions under small perturbation of the Hamiltonian. *Dokl. Akad. Nauk SSSR*, **98**:527, (1954).

S. B. Kuksin. On the inclusion of an almost integrable analytic symplectomorphism into a Hamiltonian flow. *Russian Journal of Math. Phys.*, **1**:191–207 (1993).

S. B. Kuksin and J. Pöschel. On the inclusion of analytic symplectic maps in analytic Hamiltonian flows and its applications. *Nonlinear Differential Equations Appl.*, **12**: 96–116 (1994).

E. Lega, M. Guzzo and C. Froeschlé. Detection of Arnold diffusion in Hamiltonian systems. *Physica D*, **182**:179–187 (2003).

A. Morbidelli and A. Giorgilli. Super-exponential stability of KAM tori. *J. Stat. Phys*, **78**:1607, (1995).

A. Morbidelli. *Modern Celestial Mechanics. Aspects of Solar System Dynamics.* Taylor and Francis (2002).

A. Morbidelli and A. Giorgilli. On a connection between KAM and Nekhoroshev's theorems. *Physica D*, **86**:514–516 (1995).

J. Moser. On invariant curves of area-preserving maps of an annulus. *Comm. on Pure and Appl. Math.*, **11**:81–114, (1958).

N.N. Nekhoroshev. Exponential estimates of the stability time of near–integrable Hamiltonian systems. *Russ. Math. Surveys*, **32**:1–65, (1977).

J. Poschel *Math. Z.*, Nekhoroshev estimates for quasi–convex Hamiltonian systems. **213**:187, (1993).

M. Vergassola " Standard and anomalous diffusion in dynamical systems" in Analysis and Modeling of discrete dynamical systems. Edited by D. Benest and C. Froeschlé. Gordon and Breach Science Publishers (1998).

N. Voglis, G. Contopouls, Invariant spectra of orbits in dynamical systems. *J.Phys. A:math. Gen.*, **27**, 4899–4909, (1994).